Plane-Wave Density Functional Theory Study on the Structural and Energetic Properties of Cation-Disordered Mg−Al Layered Double Hydroxides

Hong Yan,[†] Min Wei,*[,†] Jing Ma,[‡] David G. Evans,[†] and Xue Duan[†]

State Key Laboratory of Chemical Resource Engineering, Beijing University of Chemical Technology, Beijing 100029, P. R. China, and School of Chemistry and Chemical Engineering, Key Laboratory of Mesoscopic Chemistry of MOE, Nanjing University, Nanjing 210093, P.R. China

Received: December 22, 2009; Revised Manuscript Received: May 18, 2010

Periodic solid models have been employed to investigate the structural and energetic properties of cation-disordered Mg−Al layered double hydroxides (LDHs), including composition, ordering, and stacking pattern of layers. The geometry, lattice energy and density of states (DOS) of the periodic models were computed using the plane-wave pseudopotential implementation of density functional theory (DFT) with the virtual crystal approximation (VCA). The calculation results for the MgAl-Cl-LDH model show that a pure LDH phase is difficult to sustain when the Mg/Al ratio (R) is $R \geq 4$. The stability of the cation-disordered MgAl-Cl-LDH unit cell increases upon increasing R, owing to the decrease in the number of Al(III)−O−Al(III) linkages in the LDH sheets. The highest occupied molecular orbital (HOMO) and lowest unoccupied molecular orbital (LUMO) of MgAl-Cl-LDH receive contributions from the 3s and 3p orbitals of Mg and Al and the 2p orbitals of O and Cl, respectively, implying significant host−guest interactions. The increase of R leads to the decrease in electron density of 3s and 3p of metal cation and that of 2p in Cl. Consequently, the HOMO−LUMO energy gap as well as the systematical stability increase upon increasing R. From this point of view, it has been demonstrated that the cations distribute in an ordered arrangement with the absence of Al(III)−O−Al(III) linkages if R is in the low range ($R = 2-3$). It was also found that the 3R polytype is the most stable stacking pattern with the same Mg/Al ratio, owing to the fact that the conductive band energy levels decline with the increase of electron density of 3s and 3p of the metal cation in the 3R-stacking system. These findings agree well with the experimental results and provide a profound understanding of critical factors influencing the structure of LDHs, including metal composition and ordering, the stacking sequence, as well as the host−guest interactions.

Introduction

Layered double hydroxides (LDHs), also known as anionic clays, are a family of natural or synthetic host−guest layered materials that have received considerable attention recently due to their potential applications in the fields of catalysis,[1a] molecular reservoir,[1b] optical materials,[1c] functional hybrid nanostructured materials,[1d] controlled drug-release systems[1e] and thin films.[1f−j] The LDHs are generally formulated as $[M^{2+}_{1-x}M^{3+}_{x}(OH)_2]^{x+}(A^{n-}_{x/n})\cdot mH_2O$, where M^{2+} and M^{3+} stand for the di- and trivalent metal cations that occupy octahedral positions in brucite-like hydroxide layers, respectively; x is the molar ratio $M^{3+}/(M^{2+}+M^{3+})$, and A denotes interlayer charge-compensating anions.[2−4] On the basis of the variation of M^{2+}, M^{3+}, x and A^{n-} over a wide range, LDHs therefore serve as a good template for the formation of functional composite materials by host−guest structural design and assembly. The species, composition and ordering of the metallic cations, stacking sequence of layers, size and orientation of the guest, as well as the interactions between the negatively charged guest and the positively charged LDH layers are all critical factors influencing the structure of LDHs and thus determining the specific applications of these materials.

The parent material of LDHs is the naturally occurring mineral hydrotalcite with the formula $Mg_6Al_2(OH)_{16}CO_3\cdot 4H_2O$.[2] MgAl-LDH is also one of the most common synthetic LDHs.[2−4] Although the first detailed structural analysis of MgAl-LDHs was carried out in the late 1960s,[5] many structural details have not been fully understood till now: (1) The range of possible cationic compositions and stoichiometry for the pure LDH phase. It has been reported that pure LDH can be obtained in the range $0.20 < x < 0.33$ (Mg/Al ratio $R = 2-4$) in the case of natural MgAl-LDH.[2] Nevertheless, Schaper et al. reported pristine MgAl-LDH phase with x as low as 0.16 (Mg/Al = 5) using a carefully controlled coprecipitation procedure.[6] (2) The ordering of metal cations within the layers. The presence of long-range cation ordering is still a matter of debate.[7a,b] Although ordering should occur according to the cation avoidance rule,[7c] it is not experimentally observed by powder X-ray diffraction (XRD), except in the CaAl and LiAl system.[7d,e] Recently, Greenwell et al.[7f] and Evans et al.[4] summarized that extended X-ray absorption fine structure (EXAFS) studies have confirmed the local ordering with the absence of $M^{III}-O-M^{III}$ linkage in MgFe, CuCr, and MgCr LDHs.[7a,g,h] In the case of MgAl-LDHs, Gray and co-workers demonstrated the short-range order effects by the use of solid-state NMR technique.[7i] (3) The stacking sequence of the layers. Naturally occurring CO_3^{2-} containing LDHs exist as both a three-layer rhombohedral polytype hydrotalcite (the 3R polytype) and a two-layer hexagonal polytype manasseite (the 2H polytype).[8a] However, no example

* Corresponding author. Phone: +86-10-64412131. Fax: +86-10-64425385. E-mail: weimin@mail.buct.edu.cn.
[†] Beijing University of Chemical Technology.
[‡] Nanjing University.

10.1021/jp9121003
Published on Web 06/15/2010

of the 2H polytype has been prepared among the large number of synthetic LDHs unless under high preparation pressure.[8b,9]

Owing to the intrinsic relationship between LDH properties and their specific structures, recognition and understanding the microstructure of LDHs are necessary for the functionality achievement as well as extensive application of LDH materials. However, the determination of LDH structure mentioned above using experimental methods is rarely possible,[10,11] due to the inherent structural disorder and generally low crystallinity of LDH materials. With recent advances in computational software and hardware, theoretical calculation is a feasible technique to extend the study scope of these materials beyond experimental observations. A number of force-field based simulations[12] and quantum chemical calculations[13−15] were reported on the modeling of LDHs to study some specific properties related to the interlayer anions as well as the electronic structure inside LDH host layers.

Our previous theoretical work was concentrated on investigating the structure and property of host layers of LDHs using cluster models.[16] Although cluster approach gives highly accurate computations of systematic energies and electronic structures of the local properties of solids, it is not suitable for modeling the properties of the infinite crystal lattice. Recently, the plane-wave density functional theory (PW-DFT)[13a] method was applied in the study of LDHs and some clay systems, for the purpose of gaining insight into the lamella structure,[17−20] sorption and thermal behavior,[21,22] reactivity for environmental remediation,[18,23,24] interlayer water structure, and dynamics.[20,25−27]

In the present work, the PW-DFT calculations were performed to study the structure and electronic and energetic properties of the MgAl-Cl LDH using a periodic solid model. On the basis of the DFT calculation, the composition and ordering of metal cations within the host layers, the lattice stacking sequence, and the host−guest interactions, which affect the structure and stability of LDHs crucially, were systematically investigated. It was found that the 3R polytype is the most stable stacking pattern with the same Mg/Al ratio, and the cations in LDH layers are in an ordered arrangement with $R = 2-3$. The results of theoretical calculation in this work are in accordance with the experimental facts and provide fundamental information on several problems that have not been clarified by experimental techniques, including the Mg/Al ratio range in a pure MgAl-LDH phase, the cation ordering, and the stable stacking sequence for LDH structure.

Computational Details

Computational Model. The computational model of disordered MgAl-Cl LDH formulated as $Mg_{1-x}Al_x(OH)_2Cl_x$ (Mg/Al $= R = (1-x)/x = 2-5$) was constructed. For the 3R polytype, the model was built using the atomic coordinates of the naturally occurring mineral hydrotalcite ($(Mg_4Al_2(OH)_{12}CO_3(H_2O)_3)_{0.5}$).[28] The space group of 3R model is $R3\bar{m}$, with the unit cell parameters $a = b = 0.3142$ nm, $c = 2.281$ nm, $\alpha = \beta = 90°$, $\gamma = 120°$ (Figure 1A1). The 2H-polytyped model was constructed using the atomic coordinates of naturally occurring sjöegrenite ($(Mg_6Fe_2(OH)_{16}(CO_3)(H_2O)_{4.5})_{0.25}$),[29a] with the unit cell parameters of manasseite $Mg_6Al_2(OH)_{16}CO_3(H_2O)_4$: $a = b = 0.3100$ nm, $c = 1.560$ nm, $\alpha = \beta = 90°$, $\gamma = 120°$, $P63/mmc$ space group (Figure 1B1).[30a] The single-layered 1H[8a] model was also established for comparison. The parameters of the 1H model were obtained by the X-ray crystallographic data of brucite: $a = b = 0.3142$ nm, $c = 0.4766$ nm, $\alpha = \beta = 90°$, $\gamma = 120°$, $P3\bar{m}1$ space group (Figure 1C1).[31]

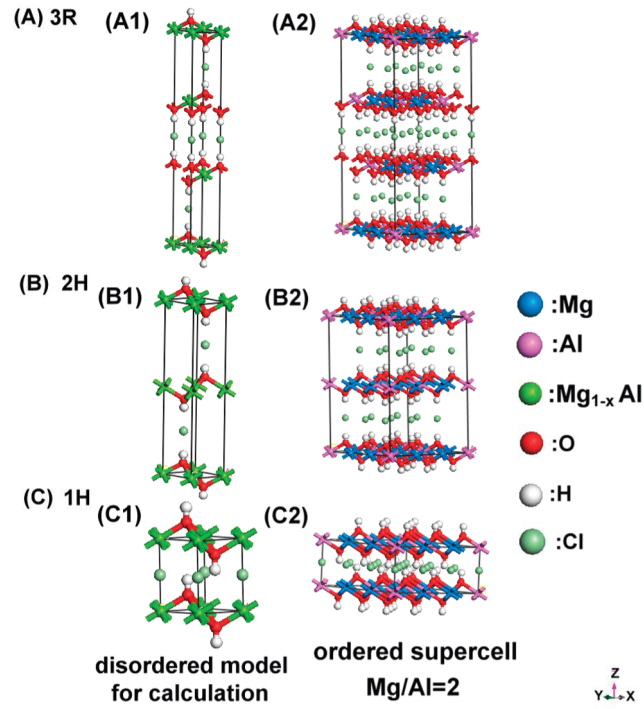

Figure 1. The periodic disordered computational model formulated as $Mg_{1-x}Al_x(OH)_2Cl_x$ and ordered $3 \times 3 \times 1$ supercells (Mg/Al ratio = 2) for MgAl-Cl-LDHs with different stacking sequences: (A) 3R; (B) 2H; (C) 1H.

Computational Method. All calculations were performed with the plane-wave pseudopotential implementation of density-functional theory[32] using the CASTEP code.[33] The ionic cores were described by ultrasoft pseudopotentials,[34] which improve transferability and reduce the number of plane waves required in the expansion of the Kohn−Sham orbitals. The Broyden−Fletcher−Goldfarb−Shanno (BFGS) algorithm was used to search the potential energy surface during optimization.[35] All structures including both cell parameters and ionic positions were fully optimized so as to obtain the minimum total energies and determine the equilibrium atomic positions and the lattice constants.

There are two fundamentally different methods to simulate the periodic crystals.[36a] The first is the so-called "configurational approach", which employs the supercells to specify the distribution of the atomic species and to calculate the structural parameters, the physical properties, and the energetics of the ordering process. Such calculations generally require the use of very large supercells in order to mimic the distribution of local chemical environments, which tend to be computationally very demanding. The second is to employ the virtual crystal approximation (VCA), which is simpler and computationally less expensive.[36b] The VCA is an average potential approximation that ignores any possible short-range order, based on the assumption that there is a virtual atom interpolating between the behavior of the actual components at each potentially disordered site. This technique has been used in the structure and property calculation for some solid solutions.[36b−d] In this work, we used the VCA to explore the properties of the cation-disordered MgAl-Cl LDHs formulated as $Mg_{1-x}Al_x(OH)_2Cl_x$, in which the ionic pseudopotential for $Mg_{1-x}Al_x$ is approximated by the weighted average of Mg and Al (Figure 1A1,B1,C1).

Results and Discussion

Selection of Proper Exchange-Correlation Functional. In order to select the most appropriate exchange-correlation

TABLE 1: The Calculated and Experimental Unit Cell Parameters of the Optimized Brucite Structure

exchange-correlation functional	cutoff energy/eV	k-points mesh	unit cell parameter		
			a,*b*/nm	*c* /nm	*V* /nm^3
GGA/PBE	310	7 × 7 × 4	0.3227	0.5380	0.04853
	340	7 × 7 × 4	0.3215	0.4802	0.04299
	380	9 × 9 × 4	0.3212	0.4786	0.04276
GGA/PW91	310	7 × 7 × 4	0.3220	0.5450	0.04894
	340	7 × 7 × 4	0.3209	0.4840	0.04317
	380	9 × 9 × 4	0.3205	0.4775	0.04248
GGA/RPBE	310	7 × 7 × 4	0.3276	0.8219	0.07639
	380	9 × 9 × 4	0.3244	0.5357	0.04883
LDA/CA-PZ	310	7 × 7 × 4	0.3134	0.4579	0.03896
	380	9 × 9 × 4	0.3129	0.4460	0.03781
exptl[31]			0.3142	0.4766	0.04075

TABLE 2: Optimized Unit Cell Parameters, Total Energies (*E*), and Lattice Energies ($\Delta E_{lattice}$) of the Disordered MgAl-Cl-LDH Model with Various Mg/Al Ratios (*R*) and Polytypes, Along with the Experimental Parameters

polytype	formula	*R*	unit cell parameter			energy	
			a,*b* /nm	*c* /nm	*V* /nm^3	*E*/eV	$\Delta E_{lattice}$/eV
3R	$Mg_2Al(OH)_6Cl$	2	0.2782	3.421	0.2293	−5915.5	−763.1
	$Mg_{2.25}Al_{0.75}(OH)_6Cl_{0.75}$	3	0.2924	3.040	0.2250	−6151.1	−871.5
	$Mg_{2.4}Al_{0.6}(OH)_6Cl_{0.6}$	4	0.3144	2.890	0.2474	−6295.6	−939.6
	$Mg_{2.5}Al_{0.5}(OH)_6Cl_{0.5}$	5	0.3041	2.768	0.2216	−6393.3	−986.4
	exptl		0.3142[a]	2.281[a]2.373[d]	0.1842[a]		
2H	$Mg_{1.33}Al_{0.67}(OH)_4Cl_{0.67}$	2	0.2535	2.119	0.1175	−3944.4	−511.2
	$Mg_{1.50}Al_{0.50}(OH)_4Cl_{0.5}$	3	0.2791	1.964	0.1325	−4105.2	−583.0
	$Mg_{1.60}Al_{0.40}(OH)_4Cl_{0.4}$	4	0.3133	1.933	0.1643	−4197.1	−626.4
	$Mg_{1.67}Al_{0.33}(OH)_4Cl_{0.33}$	5	0.3038	1.836	0.1467	−4262.2	−655.9
	exptl		0.3100[b]	1.560[b]	0.1298[b]		
1H	$Mg_{0.67}Al_{0.33}(OH)_2Cl_{0.33}$	2	0.4156	0.5574	0.08335	−1972.3	−253.2
	$Mg_{0.75}Al_{0.25}(OH)_2Cl_{0.25}$	3	0.3623	0.4843	0.05511	−2051.6	−291.8
	$Mg_{0.80}Al_{0.20}(OH)_2Cl_{0.20}$	4	0.3807	0.6150	0.07723	−2098.5	−313.1
	$Mg_{0.83}Al_{0.17}(OH)_2Cl_{0.17}$	5	0.3656	0.6052	0.07012	−2130.8	−330.2
	exptl		0.3142[c]	0.4766[c]	0.04075[c]	−1890.0[e]	

[a] Data of hydrotalcite ($(Mg_4Al_2(OH)_{12}CO_3(H_2O)_3)_{0.5}$) (ref 28). [b] Data of manasseite ($Mg_6Al_2(OH)_{16}CO_3(H_2O)_4$) (ref 30a). [c] Data of brucite ($Mg(OH)_2$) (ref 31). [d] Data of Mg_2Al-Cl-LDH (ref 29b). [e] Calculated value of brucite.

functional for simulating the MgAl-Cl-LDH system, the preliminary geometry optimizations of a unit cell of brucite, whose structure has been solved by single-crystal XRD,[31] were performed using a local density approximation (LDA)[37] and three gradient-corrected approximations (GGAs, including PW91, PBE, and RPBE functionals),[38] respectively. The calculated unit cell parameters of the optimized brucite structure with different exchange-correlation functional, plane-wave cutoff energy, and k-points mesh are listed in Table 1. All the unit cell angles show no changes during the optimizations. Comparison between the optimized structures and experimental data indicated that the LDA method overestimated bonding generally, leading to a commensurate reduction in cell parameters by 4.3% when cutoff energy is 380 eV. The PBE and PW91 functionals result in overestimation of the cell volume by 4.5−5.9%, and the former is more robust when the cutoff energy increases from 340 to 380 eV. The RPBE potential was found to typically overestimate cell parameters with an increased volume of up to 19%. These results are in agreement with those reported by Greenwell et al.[13b]

From the validation described here and prior work, the PBE potential was used for the calculation of MgAl-Cl-LDH. The cutoff energy for the plane-wave expansion was set to be 340 eV to save the computation cost. The maximum k-point spacing used was no larger than 0.04 Å^{-1}, corresponding to a 8 × 8 × 2 k-point mesh for the unit cell of MgAl-LDH.

Applicability of the VCA to the MgAl-Cl-LDHs. As mentioned above, we used the VCA to explore the properties of the cation-disordered MgAl-Cl-LDHs. Since the VCA model does not involve the relaxation around a site of substitution, a set of supercells with particular atomic arrangements and different sizes including 3 × 3 × 1 with Mg/Al ratio = 2 (Figure 1B2,C2, Figure S1C, Supporting Information), 2 × 2 × 1 with Mg/Al ratio = 3 (Figure S1A) and 2 × 3 × 1 with Mg/Al ratio = 5 (Figure S1B) were chosen to mimic the MgAl-Cl-LDHs, with the same calculation accuracy as used in the VCA. These calculations were performed for 1H and 2H polytypes, and the corresponding results are listed in Tables S1 and S2, respectively, along with the VCA results for comparison. The calculated unit cell parameters and geometries agree well with those reported by Trave et al.[13d] For the relaxed supercells, although the unit cell parameters show differences from those calculated by the VCA especially for 1H polytype, the trend is identical. On the other hand, owing to the ordered cationic arrangement of Mg and Al in the supercell models, M−O lengths and O−M−O angles present respective values for Mg and Al, and the M−O lengths and the layer thickness (d_{layer}) show opposite trends from those obtained by the VCA. As for the anions, it was found that the distance between Cl anion and the trivalent cation (Cl···Al) is shorter than that of Cl···Mg, indicating that the Cl anion is preferentially located in the interlayer region close to the trivalent cations in the supercells. The results of VCA can not distinguish the difference between Cl···Mg and Cl···Al, but the value of Cl···M is close to the average of Cl···Mg and Cl···Al for the 2H polytype. From the viewpoint of relaxation, the results of the VCA are more rigid for the large unit cell. In the case of the lattice energies, both the results of the supercell method and VCA show that

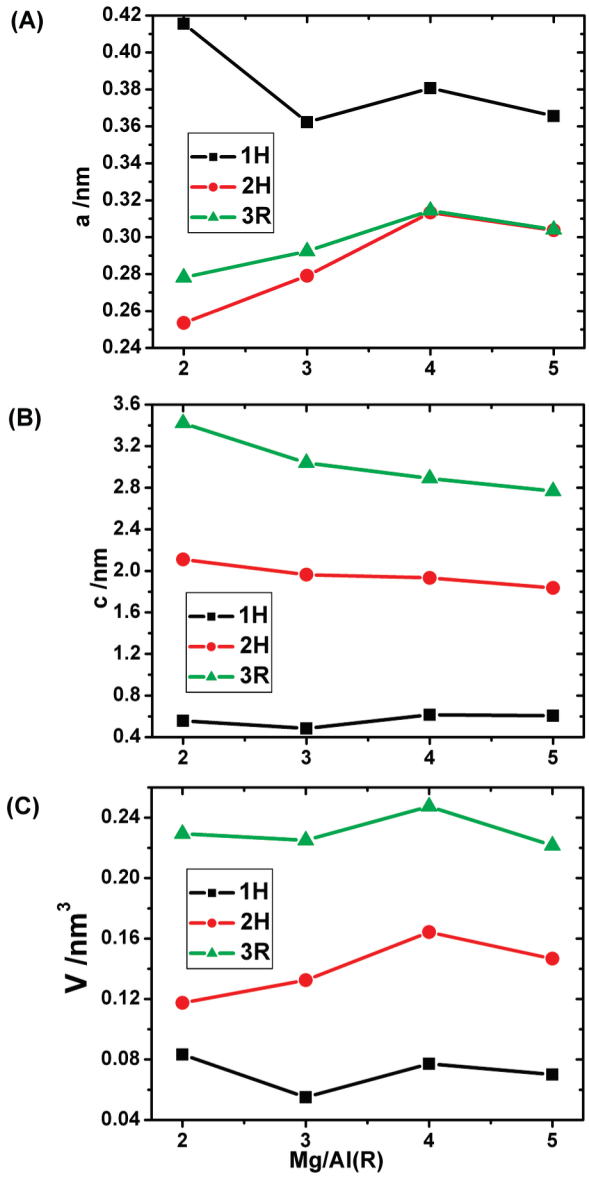

Figure 2. The optimized unit cell parameters of (A) a, (B) c, and (C) volume of the disordered MgAl-Cl-LDH model stacking in different sequences as a function of Mg/Al ratio (R).

the energy values for the 1H polytype are 2 times higher than those of the 2H polytype for the size $3 \times 3 \times 1$ or $2 \times 2 \times 1$. As a result, although the VCA can not present the same accurate geometries as those calculated by the supercell approach, it provides the same trend as the supercell method for unit cell parameters and lattice energies. Therefore, the results obtained by the VCA model are useful for studying the order/disorder and stacking stability of the MgAl-Cl-LDHs, especially for the 3R polytype, which is difficult to calculate with the supercell method.

Unit Cell Parameter. The optimized unit cell parameters of the calculated MgAl-Cl-LDHs are listed in Table 2. Figure 2 displays the relationship between the optimized unit cell parameters (a, c) and volume of the MgAl-Cl-LDH model with different stacking sequences and Mg/Al ratios (R). No change was observed for all the unit cell angles after optimization. Most of the calculated unit cell parameters are larger than the experimental data (shown in Table 2), which is related to the fact that the usage of the PBE functional leads to the overestimation of the cell parameters.

TABLE 3: Optimized Geometries of the Disordered MgAl-Cl-LDH Model Stacking in Different Sequences with Different Mg/Al Ratios (R), Along with Experimental Parameters

		bond length and interatomic distance/nm			bond angle /°
polytype	R	M−O	Cl···H	d_{layer}	O−M−O
3R	2	0.2663	0.2595	0.4247	117.01
	3	0.2357	0.2412	0.3289	103.32
	4	0.2306	0.2439	0.2846	94.07
	5	0.2220	0.2270	0.2723	93.63
exptl[28]		0.2013		0.1959	98.33
2H	2	0.2504	0.2259	0.4064	119.19
	3	0.2325	0.2249	0.3353	106.24
	4	0.2296	0.2436	0.2830	93.98
	5	0.2221	0.2245	0.2726	93.71
exptl[29a,a]		0.2060			
1H	2	0.3399	0.2473	0.4815	104.63
	3	0.2480	0.2095	0.2664	86.13
	4	0.2476	0.2397	0.2281	79.53
	5	0.2355	0.2337	0.2088	78.16
exptl[31]		0.2102		0.2112	96.70

[a] Data of sjöegrenite ($(Mg_6Fe_2(OH)_{16}(CO_3)(H_2O)_{4.5})_{0.25}$).

The unit cell parameter a of the 2H and 3R polytypes increases to a maximum with R from 2 to 4 and then declines slightly when $R = 5$ (Figure 2A). The values with $R = 4$ and 5 are close to that of brucite ($a = 0.3142$ nm), indicating the difficulty in maintaining a pure LDH phase in the range $R = 4-5$. However, the value of a in 1H stacking is larger than that of 2H or 3R. This increase is possibly caused by the smaller unit cell volume of the 1H polytype, which leads to stronger repulsion of the neighboring metal ions. The unit cell parameter c displays an equidifferent increase from 1H, 2H to 3R with the same R (Figure 2B). This finding is in accordance with the fact that LDH compounds stacked with rhombohedral symmetry present three double-layers per unit cell ($c = 3c'$, where c' is the thickness of one layer constituted by a brucite-like sheet and one interlayer); LDHs stacked with hexagonal symmetry possess two double-layers per unit cell ($c = 2c'$). The unit cell parameter c of both 2H and 3R increases with the increase of R, which is attributed to the weaker repulsion between adjacent layers when the Al content decreases. The unit cell volume with different stacking shows the same change over Mg/Al ratio (R) as that of a, reaching a maximum at $R = 4$ and then decreasing in the range $R = 4-5$. This trend indicates that the LDH phase becomes unstable, and the $Mg(OH)_2$ phase comes into formation when $R \geq 4$, leading to a smaller unit cell volume at $R = 5$. The unit cells of 3R and 1H polytypes show the smallest volume at $R = 3$, while the minimum of 2H unit cell was obtained at $R = 2$. These results agree well with the experimental facts that a pure LDH phase can be generally obtained in the range $R = 2-4$. The pure MgAl-LDHs phase with $R \geq 5$ was usually synthesized under carefully controlled conditions or sol−gel and urea hydrolysis methods,[6] since too large values of R lead to a high density of Mg octahedra in the LDH sheet facilitating the formation of $Mg(OH)_2$ or $MgCO_3$.[6b,c,10b,30b]

Geometry. Table 3 lists the optimized geometries of the MgAl-Cl-LDH. The M−O bond length decreases upon increasing R (Figure 3A), contrary to expectations based on ionic radius. This might be related to the VCA used in this study, which ignores any possible short-range order in lattice. This approximation brings about inevitable Al−O−Al linkages in the LDH lattice. The number of Al−O−Al linkages and the charge density of host layer increase with the decrease of R, resulting in stronger electrostatic repulsion of cations as well

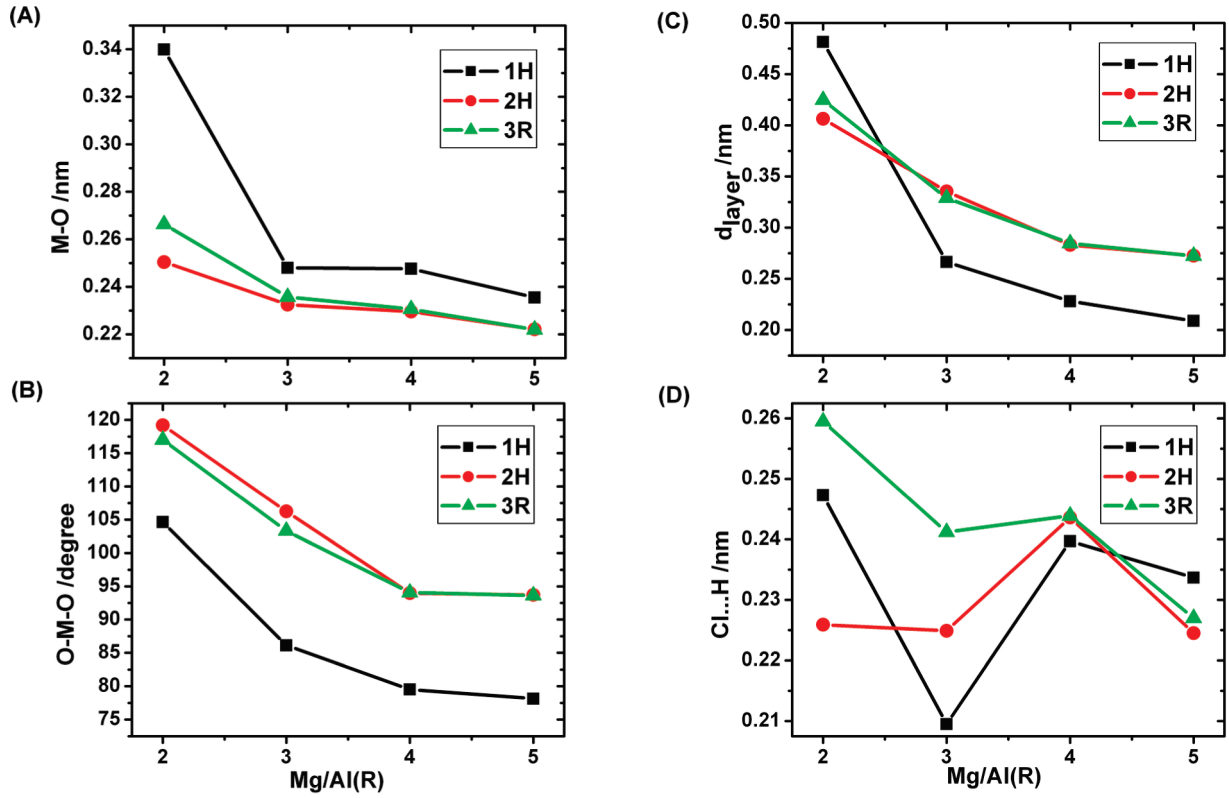

Figure 3. The optimized structural parameters of the disordered MgAl-Cl-LDH model stacking in different sequences as a function of *R*: (A) bond length; (B) bond angle; (C) lamellar thickness; (D) Cl···H distance.

as longer M−O bond length. This effect also leads to the decrease in both O−M−O bond angle (Figure 3B) and layer thickness (Figure 3C) upon increasing *R*. The Cl···H distance reflects the host−guest interactions, which shows a minimum at $R = 3$ and an inflection at $R = 4$ (Figure 3D), suggesting that the critical *R* value sustains a pure LDH phase. On the other hand, the M−O bond length of 2H and 3R polytypes is rather close, much larger than that of the 1H polytype. Both the O−M−O bond angle and layer thickness of 2H and 3R are also very close to each other. This finding is very helpful for understanding the coexistence of hydrotalcite (3R) and manasseite (2H) in nature. Manasseite generally forms the core, and hydrotalcite forms the outer part of a grain.[30b]

Lattice Energy. The lattice energies of the MgAl-Cl-LDH models were calculated in order to investigate the relative stability of the cation-disordered MgAl-Cl-LDH. On the basis of the model formula of $Mg_xAl_y(OH)_mCl_n$, the lattice energy $\Delta E_{lattice}$ of a model can be calculated as

$$\Delta E_{lattice} = E_{Mg_xAl_y(OH)_mCl_n} - xE_{Mg^{2+}} - yE_{Al^{3+}} - mE_{OH^-} - nE_{Cl^-} \quad (1)$$

where $E_{Mg_xAl_y(OH)_mCl_n}$ is the total energy of the calculated MgAl-Cl-LDH model (Table 2); $E_{Mg^{2+}} = -976.39$ eV; $E_{Al^{3+}} = -53.16$ eV; $E_{OH^-} = -454.60$ eV; $E_{Cl^-} = -413.09$ eV. The energies of ions were calculated using the same method as that of MgAl-Cl-LDH models.

The calculated lattice energies are listed in Table 2. The decrease in lattice energy of MgAl-Cl-LDH with three different polytypes upon increasing the Mg/Al ratio (*R*) is still unexpected (Figure 4). This might be due to the increase in local charge density as the result of the existing Al−O−Al linkages in the cation-disordered model. Consequently, the lattice energy of the

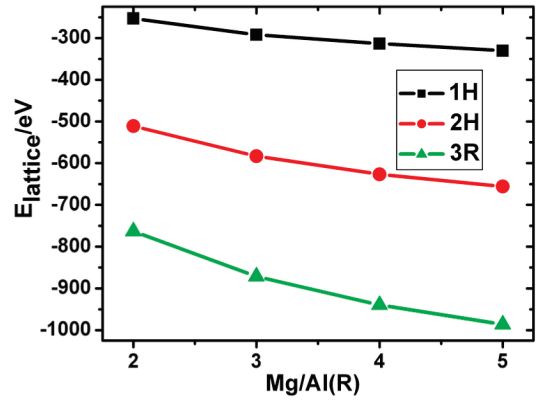

Figure 4. The lattice energy of the disordered MgAl-Cl-LDH model stacking in different sequences as a function of *R*.

LDH model decreases with the decrease in Al−O−Al bond number (i.e., the increase of *R*). From this point of view, it can be concluded that the presence of Al−O−Al linkages has a significant influence on the stability of LDH. This result also indicates that the cations prefer to be located in an ordered arrangement within the low *R* range, and the avoidance of Al−O−Al linkages is necessary for the stability of the LDH structure. This result agrees well with the recent experimental report by Sideris et al. that the cations are fully ordered in an LDH with a Mg/Al ratio of 2:1, and no $Al^{3+}-Al^{3+}$ close contacts were found with lower aluminum content.[7i]

The lattice energy of MgAl-Cl-LDH with three different polytypes shows the relationship from 1H to 3R with the same *R* value, following the order 3R > 2H > 1H. This result reveals that 3R is the most stable polytype for MgAl-LDH, while 1H is the most unstable one. This is also in accordance with the experimental fact that the 2H and 1H polytype LDH compounds can only be obtained with high preparation pressure.[9,39]

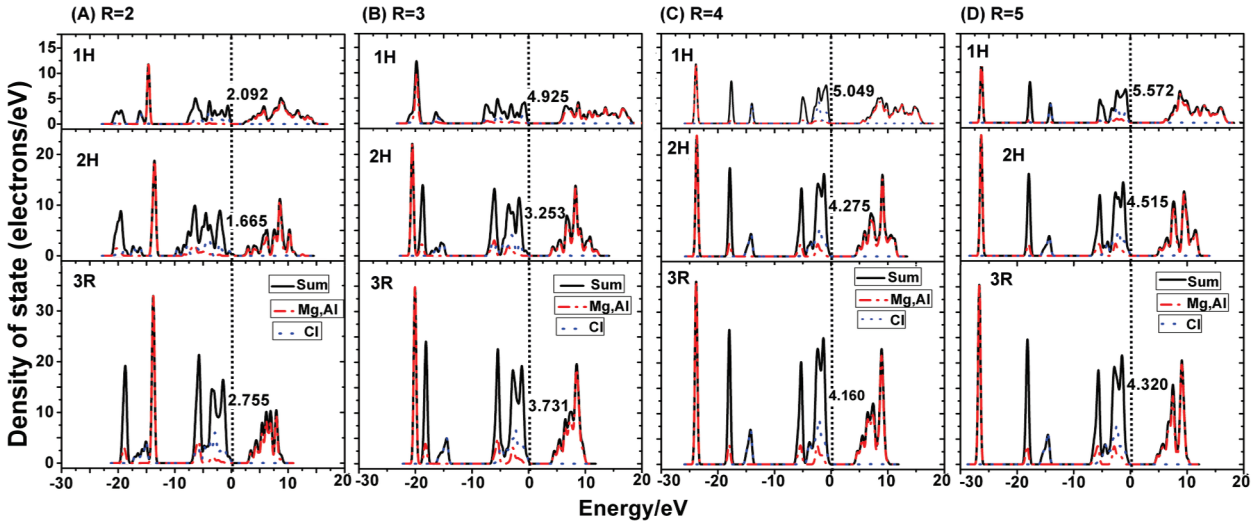

Figure 5. The TDOS and LDOS of metal cations and chloride anion of the disordered MgAl-Cl-LDH with 1H, 2H, and 3R stacking in the *R* range 2−5. The Fermi energy is shown as a dashed vertical line.

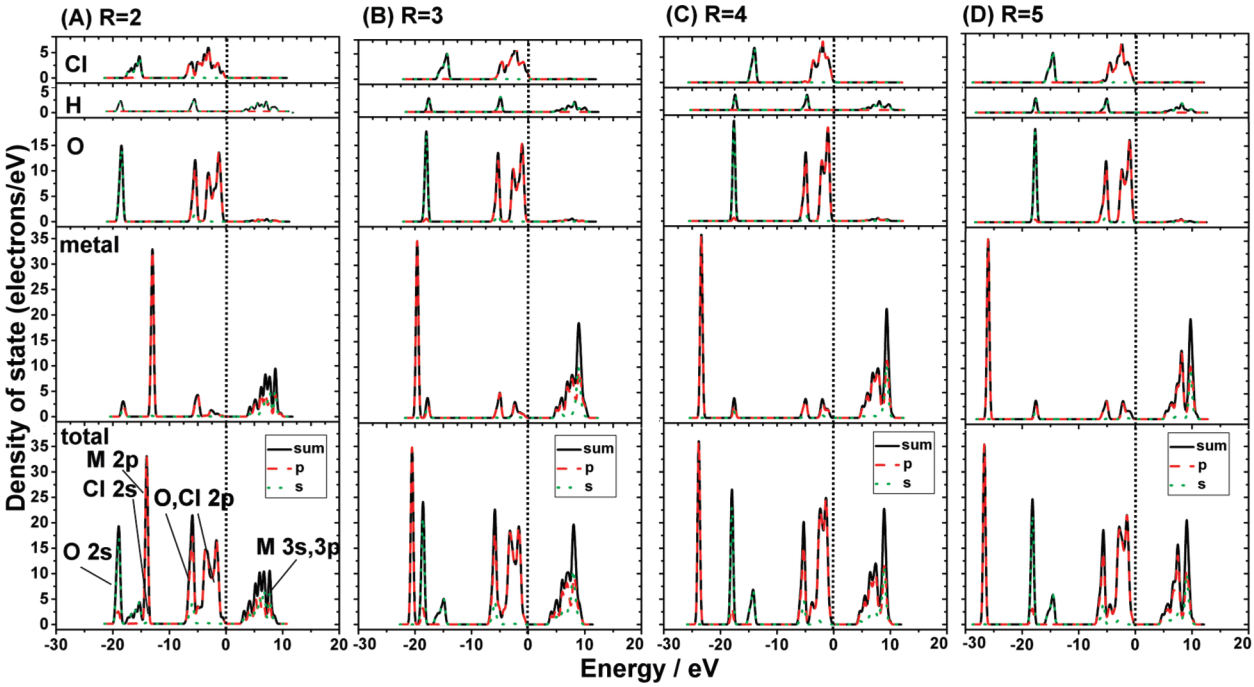

Figure 6. The PDOS of the disordered MgAl-Cl-LDH with 3R stacking in the *R* range 2−5. The Fermi energy is shown as a dashed vertical line.

Electronic Property. To obtain further electronic structural information of the effect of Mg/Al ratio (*R*) and stacking polytype on the structure of MgAl-Cl-LDH, the total density of states (TDOS) and local density of states (LDOS) of metal cations as well as chloride anion with 1H, 2H, and 3R polytypes are calculated (Figure 5). The partial density of states (PDOS) of s and p orbitals of metal, O, Cl, and H of 3R MgAl-Cl-LDH are plotted in Figure 6. The PDOS indicates the contribution of s and p states to TDOS. As shown in Figure 5 and Figure 6, the peaks in the conduction band region are mainly superimposed by a mixture of unoccupied 3s and 3p states of Mg and Al, and the peaks close to the Fermi levels in the valence band are dominated by the mixture of O 2p and Cl 2p states, indicating that the former serves as an electron acceptor, while the latter orbitals act as electron donors in the systems. This demonstrates that the host−guest interaction plays a significant role in the formation of LDH system. The other peaks in the valence band region mainly originate from metal 2p (ca. −15 eV), O 2s and Cl 2s (−20 to −15 eV), respectively.

All the MgAl-Cl-LDHs with three different stacking sequences display rather large band gaps, indicating that they are insulators (Figure 5). The band gap reflects the energy gap of the highest occupied molecular orbital (HOMO) (O and Cl 2p level) and the lowest unoccupied molecular orbital (LUMO) (Mg and Al 3s, 3p level) of the MgAl-Cl-LDH system, and a larger band gap leads to higher stability of the system. As demonstrated in Figure 5, the band gap of the MgAl-Cl-LDH system with the same polytype becomes larger as *R* increases, indicating increasingly higher stability of the system. This finding is consistent with the change of lattice energy along with *R* discussed above. It also can be seen that the increase of the band gap is caused mostly by the increase in energy of the LUMOs rather than the HOMOs.

Strong peaks were observed corresponding to the same energy in TDOS for different stacking MgAl-Cl-LDHs with the same R value (Figure 5). As R increases, the peaks in the conduction band region and the Cl and O 2p peaks in the valence band region become sharper and narrower for the 3R and 2H polytypes, and a peak of 3s appears when R is greater than or equal to 3, indicating that the dislocation of metal 3s and 3p electrons becomes weaker. These changes are attributed to the increase of the energy gap upon increasing R. The metal 2p level decreases from −15 to −27 eV with the increase of R, also due to the decrease in 2p electronic density as the Al content decreases.

As can be seen from Figure 5, the height of the peaks occurring at the same energy in TDOS with the same R value follows the order 3R > 2H > 1H. Furthermore, the peak height increases in an equidifferent relationship from 1H to 3R polytype. For example, the highest peak in the valence band region of TDOS is about 12 electrons/eV for 1H, 24 electrons/eV for 2H, and 36 electrons/eV for 3R. This difference is in accordance with different layer numbers in the unit cell for different polytypes and further demonstrates the results discussed above for unit cell parameter c. The height of the peaks in the conduction band region of TDOS increases, while their energy decreases with the increase of the stacking layers. This result suggests that the energy level of LUMO decreases with the stacking number of layers, resulting in the highest stability of 3R polytype among the three polytyes.

Conclusions

Plane-wave pseudopotential implementation of density-functional theoretical calculation was performed on periodic models of MgAl-Cl-LDH unit cells with three different stacking sequences (3R, 2H, 1H), for investigating the structural and energetic properties of cation-disordered Mg−Al LDHs. The structure of the unit cell, lattice energy, and state density of the MgAl-LDHs models were systemically discussed so as to understand the effect of cationic composition, ordering, as well as stacking pattern on the structural and energetic properties of MgAl-LDHs.

The calculation of MgAl-Cl-LDH shows that a pure LDH phase is difficult to form when R (Mg/Al ratio) is larger than 4. The stability of the cation-disordered MgAl-Cl-LDH unit cell increases upon increasing R due to the decrease of inevitable Al−O−Al linkages with R in the computational model. The HOMO and LUMO of MgAl-Cl-LDH originate from the 3s and 3p orbitals of Mg and Al and the 2p orbitals of O and Cl, respectively, implying the significant host−guest interactions. The increase of R leads to an increase in the HOMO−LUMO energy gap as well as the systematical stability, indicating cation ordering in LDH layers with low R range ($R = 2-3$). The calculation results also reveal that the system with the 3R polytype is the most stable one with the same Mg/Al ratio, which is because the conductive band energy levels decline with the increase in electron density of the 3s, 3p of metal cations.

The theoretical calculations in this work not only provide fundamental information of LDH structure on the scale of electronics, but also clarify some unclear experimental facts. This work therefore will be helpful for understanding the LDHs structure and giving a clear hint for the design and preparation of LDHs or related materials with prospective applications.

Acknowledgment. This work was supported by the National Natural Science Foundation of China, the 111 Project (Grant No. B07004), the 973 Program (Grant No. 2009CB939802), and the Fundamental Research Funds for the Central Universities (Grant No. ZZ0908).

Supporting Information Available: Views of the *ab* plane of the periodic ordered supercells with different sizes and Mg/Al ratios (Figure S1); Comparison studies of the optimized unit cell parameters, total energies (E) and lattice energies ($\Delta E_{\text{lattice}}$) for the VCA and supercell model respectively, along with the experimental parameters (Table S1); Comparisons of the optimized geometries for the VCA and supercell model respectively, along with the experimental parameters (Table S2). This material is available free of charge via the Internet at http://pubs.acs.org.

References and Notes

(1) (a) Sels, B. F.; De Vos, D. E.; Jacobs, P. A. *Angew. Chem., Int. Ed.* **2005**, *44*, 310. (b) Wei, M.; Yuan, Q.; Evans, D. G.; Wang, Z.; Duan, X. *J. Mater. Chem.* **2005**, *15*, 1197. (c) Itoh, T.; Shichi, T.; Yui, T.; Takahashi, H.; Inui, Y.; Takagi, K. *J. Phys. Chem. B* **2005**, *109*, 3199. (d) Gursky, J. A.; Blough, S. D.; Luna, C.; Gomez, C.; Luevano, A. N.; Gardner, E. A. *J. Am. Chem. Soc.* **2006**, *128*, 8376. (e) Mohanambe, L.; Vasudevan, S. *J. Phys. Chem. B* **2005**, *109*, 15651. (f) Liu, Z.; Ma, R.; Osada, M.; Iyi, N.; Ebina, Y.; Takada, K.; Sasaki, T. *J. Am. Chem. Soc.* **2006**, *128*, 4872. (g) Yan, D.; Lu, J.; Wei, M.; Han, J.; Ma, J.; Li, F.; Evans, D. G.; Duan, X. *Angew. Chem., Int. Ed.* **2009**, *48*, 3073. (h) Lee, J. H.; Rhee, S.; Jung, D. Y. *J. Am. Chem. Soc.* **2007**, *129*, 3522. (i) Zhang, F.; Zhao, L.; Chen, H.; Xu, S.; Evans, D. G.; Duan, X. *Angew. Chem., Int. Ed.* **2008**, *47*, 2466. (j) Yan, D.; Lu, J.; Wei, M.; Evans, D. G.; Duan, X. *J. Phys. Chem. B* **2009**, *113*, 1381.

(2) (a) Cavani, F.; Trifirò, F.; Vaccari, A. *Catal. Today* **1991**, *11*, 173. (b) Vaccari, A. *Appl. Clay Sci.* **1999**, *14*, 161.

(3) (a) Williams, G. R.; O'Hare, D. *J. Mater. Chem.* **2006**, *16*, 3065. (b) Rives, V.; Ulibarri, M. A. *Coord. Chem. Rev.* **1999**, *181*, 61. (c) Khan, A. I.; O'Hare, D. *J. Mater. Chem.* **2002**, *12*, 3191.

(4) Duan, X.; Evans, D. G., Eds. *Layered Double Hydroxides, Structure and Bonding*; Springer: Berlin/Heidelberg, 2006; Vol. 119.

(5) (a) Allmann, R. *Acta. Crystallogr. B* **1967**, *24*, 972. (b) Taylor, H. F. W. *Mineral. Mag.* **1969**, *37*, 338. (c) Ingram, L.; Taylor, H. F. W. *Mineral. Mag.* **1967**, *36*, 465.

(6) (a) Schaper, H.; Berg-Slot, J. J.; Stork, W. H. *J. Appl. Catal.* **1989**, *54*, 79. (b) Greenwell, H. C.; Holliman, P. J.; Jones, W.; Velasco, B. V. *Catal. Today* **2006**, *114*, 397. (c) Rao, M. M.; Reddy, B. R.; Jayalakshmi, M.; Jaya, V. S.; Sridhar, B. *Mater. Res. Bull.* **2005**, *40*, 347.

(7) (a) Vucelic, M.; Jones, W.; Moggridge, G. D. *Clays Clay Miner.* **1997**, *803*, 44–45. (b) Hofmeister, W.; von Platen, H. *Cryst. Rev.* **1992**, *3*, 3. (c) Radoslovich, E. W. *Am. Mineral.* **1963**, *48*, 76. (d) Serna, C. J.; White, J. L.; Hem, S. L. *Clays Clay Miner.* **1977**, *25*, 384. (e) Serna, C. J.; Rendon, J. L.; Iglesias, J. E. *Clays Clay Miner.* **1982**, *30*, 180. (f) Greenwell, H. C.; Coveney, P. V. *Origins Life Evol. Biospheres* **2006**, *36*, 13. (g) Roussel, H.; Biois, V.; Elkaim, E.; de Roy, A.; Besse, J. P. *J. Phys. Chem. B* **2000**, *104*, 5915. (h) Bellotto, M.; Rebours, B.; Clause, O.; Lynch, J.; Bazin, D.; Elkaim, E. *J. Phys. Chem.* **1996**, *100*, 8527. (i) Sideris, P. J.; Nielsen, U. G.; Gan, Z.; Grey, C. P. *Science* **2008**, *321*, 113.

(8) (a) Bookin, A. S.; Drits, V. A. *Clays Clay Miner.* **1993**, *41*, 551. (b) Bookin, A. S.; Cherkashin, V. I.; Drits, V. A. *Clays Clay Miner.* **1993**, *41*, 558.

(9) Drits, V. A. ; Bookin, A. S. In *Layered Double Hydroxides: Present and Future*; Rives, V., Ed.; Nova Science Publishers: New York, 2001; Chapter 2.

(10) (a) Vucelic, M.; Moggridge, G. D.; Jones, W. *J. Phys. Chem.* **1995**, *99*, 8328. (b) Xu, Z. P.; Zeng, H. C. *J. Phys. Chem. B* **2001**, *105*, 1743. (c) Brindley, G. W.; Kikkawa, S. *Am. Mineral.* **1979**, *64*, 836. (d) Xu, Z. P.; Zeng, H. C. *Chem. Mater.* **2001**, *13*, 4564.

(11) (a) Kooli, F.; Chisem, I. C.; Vucelic, M.; Jones, W. *Chem. Mater.* **1996**, *8*, 1969. (b) Turco, M.; Bagnasco, G.; Costantino, U.; Marmottini, F.; Montanari, T.; Ramis, G.; Busca, G. *J. Catal.* **2004**, *228*, 43. (c) Bourrié, G.; Trolard, F.; Refait, P.; Feder, F. *Clays Clay Miner.* **2004**, *52*, 382.

(12) (a) Greenwell, H. C.; Jones, W.; Coveney, P. V.; Stackhouse, S. *J. Mater. Chem.* **2006**, *16*, 708. (b) Lombardo, G. M.; Pappalardo, G. C.; Punzo, F.; Costantino, F.; Costantino, U.; Sisani, M. *Eur. J. Inorg. Chem.* **2005**, 5026. (c) Mohanambe, L.; Vasudevan, S. *J. Phys. Chem. B* **2005**, *109*, 15651. (d) Kalinichev, A. G.; Kirkpatrick, R. J. *Chem. Mater.* **2002**, *14*, 3539. (e) Greenwell, H. C.; Jones, W.; Newman, S. P.; Coveney, P. V. *J. Mol. Struct.* **2003**, *647*, 75. (f) Mohanambe, L.; Vasudevan, S. *Langmuir* **2005**, *21*, 10735. (g) Kumar, P. P.; Kalinichev, A. G.; Kirkpatrick, R. J. *J. Phys. Chem. B* **2006**, *110*, 3841. (h) Newman, S. P.; Williams, S. J.; Coveney, P. V.; Jones, W. *J. Phys. Chem. B* **1998**, *102*, 6710. (i) Wang, J. W.; Kalinichev, A. G.; Kirkpatrick, R. J.; Hou, X. *Chem. Mater.* **2001**, *13*, 145. (j) Cygan, R. T.; Liang, J. J.; Kalinichev, A. G. *J. Phys. Chem. B*

2004, *108*, 1255. (k) Aicken, A. M.; Bell, I. S.; Coveney, P. V.; Jones, W. *Adv. Mater.* **1997**, *9*, 409. (l) Li, H.; Ma, J.; Evans, D. G.; Zhou, T.; Li, F.; Duan, X. *Chem. Mater.* **2006**, *18*, 4405. (m) Thyveetil, M. A.; Coveney, P. V.; Greenwell, H. C.; Suter, J. L. *J. Am. Chem. Soc.* **2008**, *130*, 4742. (n) Hou, X.; Kirkpatrick, R. J. *Chem. Mater.* **2002**, *14*, 1195.

(13) (a) Stackhouse, S.; Coveney, P. V.; Sandre, E. *J. Am. Chem. Soc.* **2001**, *123*, 11764. (b) Greenwell, H. C.; Stackhouse, S.; Coveney, P. V.; Jones, W. *J. Phys. Chem. B* **2003**, *107*, 3476. (c) Refson, K.; Park, S. H.; Sposito, G. *J. Phys. Chem. B* **2003**, *107*, 13376. (d) Trave, A.; Selloni, A.; Goursot, A.; Tichit, D.; Weber, J. *J. Phys. Chem. B* **2002**, *106*, 12291.

(14) (a) Gorb, L. G.; Aksenenko, E. V.; Adams, J. W.; Larson, S. W.; Weiss, C. A.; Leszczynska, D.; Leszczynski, J. *J. Mol. Struct.* **1998**, *425*, 129. (b) Scholtzová, E.; Tunega, D.; Nagy, L. T. *J. Mol. Struct. (THEOCHEM)* **2003**, *620*, 1. (c) Aronowitz, S.; Coyne, L.; Lawless, J.; Rishpon, J. *Inorg. Chem.* **1982**, *21*, 3589.

(15) (a) Peterson, R. C.; Hill, R. J.; Gibbss, G. V. *Can. Mineral.* **1979**, *17*, 703. (b) Pu, M.; Zhang, B. *Mater. Lett.* **2005**, *59*, 3343. (c) Sato, H.; Morita, A.; Ono, K.; Nakano, H.; Wakabayashi, N.; Yamagishi, A. *Langmuir* **2003**, *19*, 7120. (d) Sainz-Diaz, C. I.; Timon, V.; Botella, V.; Hernandez-Laguna, A. *Am. Mineral.* **2000**, *85*, 1038.

(16) (a) Yan, H.; Lu, J.; Wei, M.; Ma, J.; Li, H.; He, J.; Evans, D. G.; Duan, X. *J. Mol. Struct. (THEOCHEM)* **2008**, *866*, 34. (b) Yan, H.; Wei, M.; Ma, J.; Li, F.; Evans, D. G.; Duan, X. *J. Phys. Chem. A* **2009**, *113*, 6133.

(17) Chatterjee, A.; Iwasaki, T.; Ebina, T.; Miyamoto, A. *Comput. Mater. Sci.* **1999**, *14*, 119.

(18) Teppen, B. J.; Yu, C.-H.; Newton, S. Q.; Miller, D. M.; Schäffer, L. *J. Phys. Chem. A* **2002**, *106*, 5498.

(19) Benco, L.; Tunega, D.; Hafner, J.; Lishka, H. *Am. Mineral.* **2001**, *86*, 1057.

(20) Bridgeman, C. H.; Buckingham, A. D.; Skipper, N. T.; Payne, M. C. *Mol. Phys.* **1996**, *89*, 879.

(21) Churakov, S. V. *J. Phys. Chem. B* **2006**, *110*, 4135.

(22) Stackhouse, S.; Coveney, P. V. *J. Phys. Chem. B* **2002**, *106*, 12470.

(23) Stackhouse, S.; Coveney, P. V.; Benoit, D. M. *J. Phys. Chem. B* **2004**, *108*, 9685.

(24) Gorb, G. L.; Gu, J.; Leszczynska, D.; Leszczynski, J. *Phys. Chem. Chem. Phys.* **2000**, *2*, 5007.

(25) Tunega, D.; Benco, L.; Haberhauer, G.; Gerzabeck, M. H.; Lischka, H. *J. Phys. Chem. B* **2002**, *106*, 11515.

(26) Chatterjee, A.; Iwasaki, T.; Ebina, T. *J. Phys. Chem. A* **2000**, *104*, 8216.

(27) Boek, E. S.; Sprik, M. *J. Phys. Chem. B* **2003**, *107*, 3251.

(28) Allmann, R.; Jepsen, H. P. *Neues Jahrb. Mineral., Monatsh.* **1969**, 544.

(29) (a) Allmann, R. *Neues Jahrb. Mineral., Monatsh.* **1969**, 552. (b) Boclair, J. W.; Braterma, P. S. *Chem. Mater.* **1999**, *11*, 298.

(30) (a) Taylor, H. F. W. *Miner. Mag.* **1973**, *39*, 377. (b) Pausch, I.; Lohse, H.-H.; Schirmann, K.; Allmann, R. *Clays Clay Miner.* **1986**, *34*, 507.

(31) Ziagan, F.; Rothbauer, R. *Neues Jahrb. Mineral., Monatsh.* **1967**, *4*, 137.

(32) Payne, M. C.; Teter, M. P.; Allan, D. C.; Arias, T. A.; Joannopoulos, J. D. *Rev. Mod. Phys.* **1992**, *64*, 1045.

(33) (a) Segall, M. D.; Lindan, P. L. D.; Probert, M. J.; Pickard, C. J.; Hasnip, P. J.; Clark, M. C.; Payne, M. C. *J. Phys. (Paris)* **2002**, *14*, 2717. (b) Segall, M.; Probert, M.; Pickard, C.; Hasnip, P.; Clark, S.; Refson, K.; Payne, M. *CASTEP Module, MS Modeling*, version 2.2; Accelrys Inc.: San, Diego, CA, 2003.

(34) Vanderbilt, D. *Phys. Rev. B* **1990**, *41*, 7892.

(35) Press, W. H.; Teukolsky, S. A.; Vetterling, W. T.; Flannery, B. P. *Numerical Recipes*, 2nd ed.; Cambridge University Press: Cambridge, 1992.

(36) (a) Winkler, B.; Pickard, C.; Milman, V. *Chem. Phys. Lett.* **2002**, *362*, 266. (b) Bellaiche, L.; Vanderbilt, D. *Phys. Rev. B* **2000**, *61*, 7877. (c) Ramer, N. J.; Rappe, A. M. *Phys. Rev. B* **2000**, *62*, 743. (d) Jhi, S.-H.; Ihm, J.; Louie, S. G.; Cohen, M. L. *Nature* **1999**, *399*, 132.

(37) Ceperley, D. M.; Alder, B. J. *Phys. Rev. Lett.* **1980**, *45*, 566.

(38) Perdew, J. P.; Burke, K.; Ernzerhof, M. *Phys. Rev. Lett.* **1996**, *77*, 3865.

(39) Parthasarathy, G.; Kantam, M. L.; Choudary, B. M.; Reddy, C. V. *Microporous Mesoporous Mater.* **2002**, *56*, 147.

JP9121003